Analysis of superconducting thin films in a modern FIB/SEM dual-beam instrument

Lukas Grünewald[1], Daniel Nerz[1], Marco Langer[2], Sven Meyer[2], Nico Beisig[2], Pablo Cayado[2], Ruslan Popov[2], Jens Hänisch[2], Bernhard Holzapfel[2] and Dagmar Gerthsen[3]

[1]Karlsruhe Institute of Technology (KIT), Laboratory for Electron Microscopy (LEM), Engesserstraße 7, 76131 Karlsruhe, Germany, United States, [2]Karlsruhe Institute of Technology (KIT), Institute for Technical Physics (ITEP), Hermann-von-Helmholtz-Platz 1, 76344 Eggenstein-Leopoldshafen, Germany, United States, [3]Laboratorium für Elektronenmikroskopie, Karlsruher Institut für Technologie (KIT), Engesserstr. 7, 76131 Karlsruhe, Germany, United States

Thin-film technology is used for the synthesis of many application-relevant materials, e.g. for the fabrication of superconducting thin films for high-power applications [1]. The superconducting properties of such a thin film are strongly dependent on the microstructure because structural defects can act as flux-pinning centers if they have favorable size, shape, and distribution within the superconducting matrix [2]. This increases the critical current density, which is important for technical applications. (Scanning) transmission electron microscopy ((S)TEM) in a dedicated (S)TEM instrument is a powerful analysis tool for film characterization on the sub-nm (and sub-Å) scale. However, TEM sample preparation and consecutive (S)TEM measurement in different instruments limit high-throughput analysis. Modern combined focused-ion-beam/scanning electron microscope (FIB/SEM) instruments are routinely used for TEM sample preparation and SEM imaging and can be additionally equipped with STEM- (for STEM-in-SEM imaging) and energy-dispersive x-ray spectroscopy- (EDXS) detectors, resulting in a large versatility for material analysis [3].

In this work, we demonstrate how correlative SEM, EDXS, and STEM-in-SEM in a Thermo Fisher Helios G4 FX FIB/SEM dual-beam instrument, equipped with a dedicated STEM holder and a Bruker XFlash 6|60 EDXS system, can be used for sample preparation and structural and chemical characterization within one instrument [3]. The investigated thin films consist of superconducting $Ba(Fe_{0.92}Co_{0.08})_2As_2$ (Ba122) and rare-earth barium copper oxide $REBa_2Cu_3O_{7-\delta}$ (REBCO, with RE=Y, Gd, Er, …) and are grown by pulsed laser and chemical solution deposition on different substrates.

Fig. 1 shows the SEM-EDXS analysis of a thin Ba122 film grown on CaF_2 that contains precipitates with sizes of about 80 nm (bright spots in Fig. 1(a)). EDXS mapping was performed in the region marked in Fig. 1(a) for chemical analysis of the film and the precipitates. Due to the small thickness (60 nm) of the Ba122 film, a low electron energy of 2 keV was used to maximize the spatial resolution while still exciting all necessary x-ray lines, i.e. the Ba M-line-, Fe L-line-, Co L-line, and As L-line-families. Due to the low x-ray yield at 2 keV, principal component analysis (PCA) is applied to increase the signal-to-noise ratio (Fig. 1(b)) by dimensionality reduction of the dataset [4]. The precipitates show a high Fe/Co content in the qualitative net-intensity elemental maps (Fig. 1(c)) in agreement with TEM results [5]. STEM-in-SEM imaging of Ba122 shows a reduced intensity in high-angle annular dark-field (HAADF) *Z*-contrast at planar defects (dotted arrows, Fig. 1(e)). Their dark appearance in HAADF-STEM images is similar to STEM images taken in a dedicated (S)TEM [5], where O was detected at these defects. By in-situ preparation and STEM-in-SEM imaging, it was possible to eliminate possible oxidation of these planar defects during sample transport between the FIB/SEM and the dedicated (S)TEM instrument. Ba122(002) lattice fringes are visible in the simultaneously acquired bright-field (BF) image (Fig. 1(d)), which shows that BF STEM-in-SEM imaging can resolve sub-nm crystalline features.

Examples for STEM-in-SEM imaging at 30 keV of in-situ FIB-prepared samples from a GdBCO film with a thickness of 350 nm on a MgO substrate are shown in Fig. 2. Diffraction-contrast STEM-in-SEM dark-field imaging shows vertical, out-of-plane defects in the film (Fig. 2(a)). These defects correspond to threading dislocations, antiphase boundaries, and small-angle [001]-twist grain boundaries. For a better overview of the microstructure, additional plan-view samples were prepared by FIB milling and imaged by STEM-in-SEM (Fig. 2(b,c)). HAADF-STEM images of the same GdBCO film as in (a) show roundish precipitates, twin boundaries oriented along [110]-type directions (red arrows, as in [6]), and threading dislocations (orange arrows).

In conclusion, modern FIB/SEM instruments with STEM and EDXS detectors combine sample preparation with structural and chemical analysis down to the nm-scale and facilitates efficient thin-film analysis in a single instrument. This is particularly favorable for the investigation of materials that are susceptible to exposure to ambient air.

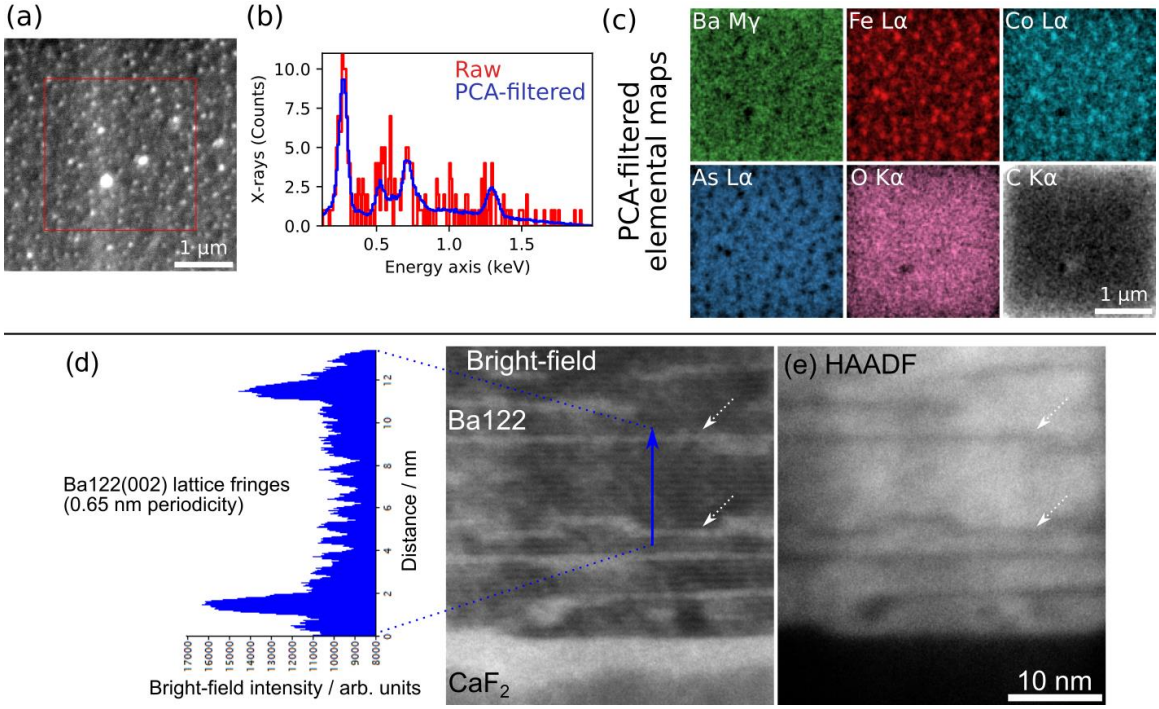

Figure 1. Low-energy SEM-EDXS analysis of a ~60 nm thin Ba122 film on CaF_2. (a) Overview secondary-electron SEM image with EDXS-mapped region marked by a square. (b) Example for raw (red) and PCA-filtered (blue) EDXS spectra from a single pixel of the EDXS dataset. The enhanced signal-to-noise ratio enables improved separation of the partially overlapping x-ray lines. (c) Extracted net intensities of the x-ray lines for different elements. The precipitates are rich in Fe and Co. (d, e) Simultaneously acquired 30 keV STEM-in-SEM (d) BF- and (e) HAADF-STEM cross-section images of a Ba122 film. The dotted arrows mark planar defects with increased/reduced intensity in the BF- and HAADF-STEM images. Ba122 lattice fringes are visible in the BF image as visible in the intensity line profile along the blue arrow.

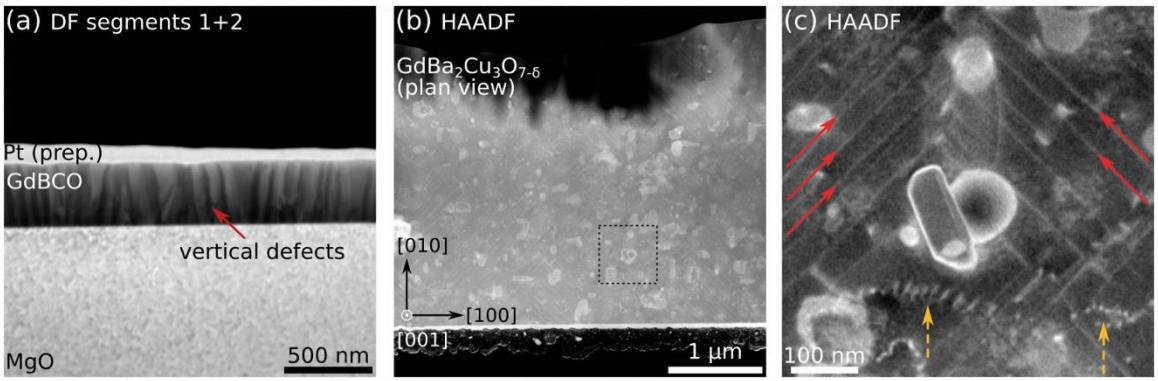

Figure 2. (a) STEM-in-SEM dark-field cross-section image of a ~350 nm thin GdBCO film. The vertical defects show strong diffraction contrast. (b, c) Plan-view HAADF-STEM-in-SEM images of an in-situ prepared plan-view lamella of the GdBCO film. (c) Higher-magnification image of the region marked in (b). Twin boundaries (red arrows) and threading dislocations (yellow, dashed arrows) are visible besides precipitates.

References

[1] A.K. Jha, K. Matsumoto, *Front. Phys.* **7** (2019) 82.
[2] J.P.F. Feighan et al., *Supercond. Sci. Technol.* **30** (2017) 123001.
[3] C. Sun et al., *J. Mater. Sci.* **55** (2020) 13824–13835.
[4] P. Potapov, *Ultramicroscopy* **160** (2016) 197–212.
[5] L. Grünewald et al., Supercond. Sci. Techno*l.* **34** (2021) 035005.
[6] R. Guzman et al., *Phys. Rev. Mater.* **1** (2017) 24801.